

A Review on Counter Electrode Materials in Dye Sensitized Solar Cell

¹T.BLESSLINE PONMANI, ²T.S.RAHUL RAJU, ³A.MOHAN VAMSI

¹Assistant. Professor, Department of chemistry

^{2,3}UG Scholar, Department of computer Science, Panimalar Engineering College

Abstract - Dye-sensitized solar cells (DSCs) present low-cost alternatives to the conventional silicon (Si)-based solar cells. The components of DSCs are metal oxide-based Photo anode, an electrolyte, a dye and a counter electrode. The photo excited electrons from the dye diffuse through the TiO₂ network in the Photo anode and reaches the Pt-counter electrode where Pt is sputtered to a fluorine-doped tin oxide (FTO) plate. Regeneration of dyes takes place by catalysis I⁻ species in the redox couple. High efficiency is determined by Pt due to its surface roughness, exposed facet, etc, with Pt being a costly noble metal, reasonable effort have been made to find cheaper alternatives. The review presented below gives a summary of materials in use as counter electrodes in DSCs, with a conclusion and future prospects section.

Key Words: Dye-sensitized solar cells, conventional silicon, fluorine-doped tin oxide, electrodes, catalysis

1.INTRODUCTION

In 1960 by Gerisher and Tributsch on a ZnO photo anode and chlorophyll as a sensitizer.^{4,5} Since the photovoltaic performance was low, more work on ZnO with dyes such as Rose Bengal and cyanine was carried out, but still the cell performance was not good, due to the instability of the dyes.^{6,7} Spitler and Calyin, in 1977, proved that TiO₂ can be used instead of ZnO, due to its high dye absorption property, which resulted in giving an excellent current density also.⁸ Grätzel and O'Regan's work on DSCs, by using nanometer sized TiO₂ particles, together with newly developed dyes by providing a better stability and improved efficiency for the cell.¹

Over the last 20 years, modifications of DSCs are ongoing to improve their photovoltaic performance. Nanomaterials play a key role in the development of DSCs.^{10,11} In general, a DSC consists of a large band-gap, n-type semiconductor electrode (photo anode), a sensitizer (dye), a redox electrolyte, and a counter electrode (CE). Starting with the photo anode, TiO₂ is a widely used photo anode material in DSCs for its many advantages, such as its availability, non-toxicity, chemical stability, etc.⁹ Nanotechnology has huge implications on DSCs, as it helped in fabricating TiO₂ of different morphologies (instead of the conventional spherical particles), such as nanofibers, nanowires, nanorods, nanowhiskers, nanotubes, nano/ mesoflowers, etc. by electrospinning, hydrothermal, and other complex processes involving structure-directing chemical methods.¹²⁻¹⁶ These nanostructures come under the category of 1-D and 3-D structures, in which the former provide direct pathways for

the rapid collection of photogenerated electrons and the latter give high surface area photoanodes, which are the backbone of DSCs. Efforts are underway to increase the surface area of TiO₂ nanostructures further, which can enhance the overall performance of DSCs. Similarly, nanomaterials hold an important role in the counter electrode of a DSC also. A platinised catalyst is used as a CE in a DSC mainly for two reasons: (1) it acts as a catalyst that helps in the regeneration of I⁻ from I₃⁻, and (2) the collection of electrons from the external load to the electrolyte. Since Pt is an extremely expensive noble metal and diminishing in its reserve, there is a need to explore Pt-free materials for the CE in DSCs. According to various research, there are many promising alternatives to Pt, including carbonaceous materials such as carbon black, carbon nanotubes (CNTs), graphene, polymers and transition metal carbides, nitrides, etc. This review provides an in-depth investigation on the exciting alternative materials as CEs in DSCs and how they enhance the overall photovoltaic performance of DSCs.

1.1 Operational principle

Fig. 1 shows the basic components of a DSC. The heart of a DSC is the mesoporous TiO₂ (anatase) nanoparticles/nanostructures deposited onto an FTO substrate with a thickness of 10-12 μm and a porosity of 50-60%. This TiO₂ layer is coated with a monolayer of a photo sensitizer (the dye). The photo excitation of electrons occurs from the HOMO (highest occupied molecular orbital) to the LUMO (lowest unoccupied molecular orbital) of the dye, followed by the injection of electrons from the LUMO level to the conduction band (CB) of the semiconductor, leaving the dye in an oxidized state. The oxidized dye is restored to its original state by electron transfer from the electrolyte, and this step is known as the dye regeneration process. Regeneration of the dye by iodide intercepts the recapture of the injected electron in the CB by the oxidized dye. The triiodide ions (I₃⁻) formed by the oxidation of iodide (I⁻) diffuse through the counter electrode usually composed of islands of finely divided Pt. The regenerative cycle is completed by the conversion of I₃⁻ to I⁻ ions. The electrical circuit is completed by the migration of electrons to the external circuit. Under light illumination (AM 1.5), a voltage is generated, corresponding to the difference of the Fermi level of the electron in the metal oxide and the redox potential of the electrolyte.^{17,18}

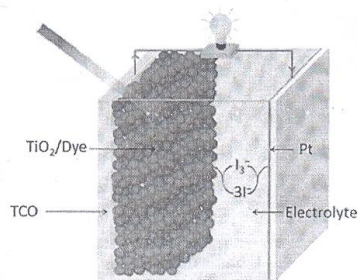


Fig. 1 A schematic of a DSC device.¹⁷

III. Electron transfer in DSCs

The exposure of DSCs to visible light leads to a sequence of chemical reactions explained in brief in Fig. 2, which illustrates the following processes.

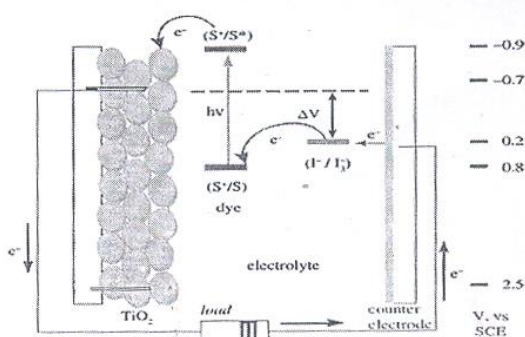


Fig. 2 Schematic diagram of a DSC showing the sequence of electron transfer.²⁷ [Adapted from *Dye Sensitized Solar Cell* by K. Kalyanasundram.]

1. Electron excitation in dye by absorption of photons and ultrafast electron injection

Under exposure to light, the dye absorbs the photons which strike the transparent conducting oxide (TCO) film. The dye absorbs those solar photons whose energy matches the HOMOLUMO energy-gap, which leads to the formation of electronically excited dye molecule [i.e. an electronic transition from the HOMO to the LUMO, The excited dye molecule can decay back to the ground state or undergo oxidative quenching by injecting an electron into the CB of the semiconductor (TiO₂). An ultra-fast electron injection to the CB of the semiconducting layer from the excited dye is one of the most astounding findings in DSCs. The charge transfer occurs via the dye-TiO₂ interfacial bond due a strong electronic coupling between the two. The timescale of this process is in tens of a femtosecond to hundreds of a picosecond range.¹⁹⁻²² The injected electrons in the CB are collected at the anode electrode in the micro- to millisecond range. The oxidized dye is regenerated back in a nanosecond timeframe. The electron charge transport and recombination in a DSC are determined by an effective carrier diffusion length (L_n). The diffusion length is largely independent on the light intensity and typically the L_n values range from 5-20 μm.⁹

2. Reactions at the counter electrode

Typically an electrolyte in a DSC comprises a I⁻/I₃⁻ redox species dissolved in an organic liquid solvent. The main function of the electrolyte is the regeneration of the oxidized dye by iodide (I⁻), the electron donor in the electrolyte. The oxidation of iodide produces I₃⁻ ions. The I₃⁻ regenerates the I⁻ by accepting electrons from the external load. In general, electrons flowing from the anode to the external load are collected at the Counter electrode. The open-circuit voltage (V_{oc}) across the cell is thermodynamically determined by the difference between the quasi-Fermi level (QFL) of the semiconductor and the redox potential of the electrolyte. More often than not, Pt is used as the counter electrode in a DSC due to its electrocatalytic activity and excellent Stability towards the I⁻/I₃⁻ electrolyte. A counter electrode must be catalytically active for a rapid reaction and reduce the overpotential. The overpotential is required to drive the reaction at a certain current density, which gives rise to a charge transfer resistance (RCT). To avoid significant losses of electrons in the counter electrode, RCT should be of 1 W cm².²³ The importance, role and composition of the CE, in detail, are detailed subsequently in the next section of this review.

3. Recombinations

The possibility of photoelectrons recombining back with the electrolyte or an oxidized dye molecule is the most probable recombination reaction. This process is also known as a back electron transfer. Mainly, two possible recombination routes are present in DSCs: the direct recombination of CB electrons in TiO₂, with oxidized dyes and with the I₃⁻ species in the electrolyte. The recombination with a dye molecule is in the order of a micro- to millisecond, whereas recombination with the electrolyte is in the range of a millisecond to second. Both these recombinations take place at the TiO₂/dye-electrolyte interface. These recombinations can be controlled by using 1-D metal oxide nanostructures as photoanodes, enhancing the conductivity of the TiO₂ nanostructures by having composites with carbon nanomaterials, effecting the necking between the TiO₂ particles by TiCl₄ treatment, and by depositing a thin layer of TiO₂ film between the FTO and nanocrystalline TiO₂ by TiCl₄, etc.²⁴⁻²⁶

4. Overall reactions in DSCs



5. Efficiency parameters of OSC

To know the overall performance of the cell, certain parameters are considered and measured under a monochromatic light source. The most important amongst them are: (1) the incident photon-to-electrical conversion efficiency (IPCE), which represents the overall charge injection process measured using a single wavelength source.

$$IPCE(\lambda) = 1240(I_{sc}/\lambda j) \quad (8)$$

where λ is the wavelength, I_{sc} is the short circuit current and j is the incident radiative flux.

(2) The overall sunlight-to-electric power conversion of a DSC is given by:

$$h = P_{max} / P_{in} = I_{sc} V_{oc} FF / P_{in} \quad (9)$$

where the maximum obtainable power (P_{max}) in a DSC is the product of I_{max} and V_{max} , P_{in} is the intensity of incident light. Similarly, the overall sunlight to electric power conversion can be expressed as the product of the three key terms:

$$H = \eta_{abs} \eta_{inj} \eta_{coll} \quad (10)$$

where η_{abs} is the efficiency of light absorption by the dye, η_{inj} is the efficiency of the charge injection from the excited state of the dye and η_{coll} is the amount of charge collection in the mesoporous oxide layer.²⁷

IV. Counter electrodes in DSCs

I. Importance and role of counter electrode

A counter electrode (CE) is one of the most important components in DSCs. The main task of the CE is that (a) it acts as a catalyst by reducing the redox species, which are the mediators for regenerating the sensitizer (dye) after the electron injection, or (b) for collecting the hole from the hole-transporting materials in a solid state DSC. Most of the research in DSCs are focused on boosting the short-circuit current density (JSC), open-circuit voltage (VOC) and fill-factor (FF) for increasing the efficiency. Normally, a Pt-coated FTO is used as a CE. By improving the CE material, the fill-factor (FF) of the cell rises, which is mainly influenced by the series resistance (R_s) of the cell which is related to the slope of the tangent line to the current density (J)-voltage (V) curve at VOC. The series resistance is a combination of the Warburg impedance relative to the Nernst diffusion of the I_3^- species in the electrolyte (Zn), which is the impedance related to charge transfer and recombination at the TiO_2 -dye-electrolyte interface (RAN), resistance at the fluorine-doped tin oxide (FTO) glass (RH), and the charge-transfer resistance at the CE and the electrolyte interface (RCT). Fig. 3 shows the equivalent circuit used to represent interfaces in

DSCs, where $R_{CT}(solid)$ is the charge transfer resistance of the TiO_2 -FTO or Pt-FTO interface, $C(solid)$ is the capacitance of the TiO_2 -FTO or Pt-FTO interface and $W(Sol)$ is the Warburg parameter describing the diffusion of the I_3^- electrolyte. Amongst all these resistances, a prominent role is handled by RCT to determine R_s . A lower value of RCT signifies tremendous electron transfer from the CE to the electrolyte for the reduction of the I_3^- ion to the I^- ion at the catalytic interfaces of the CE.

A superficial electron transfer between the CE and electrolyte reduces the series resistance (R_s), thereby giving a higher FF, which results in a high conversion efficiency.²⁸⁻³⁰ The catalytic activity of the CE can be explained in terms of the current density (f), which is calculated from the charge transfer resistance (RCT), given by the equation:

$$RCT = RT/nf \quad (11)$$

where R , T , n , and F are the gas constant, temperature, the number of electrons transferred in the elementary electrode reaction ($n = 2$) and Faradays constant,³¹ respectively.

The reactions at the CE mainly depend on the redox species used to transfer electrons between the photo anode and the CE. Usually, an I^-/I_3^- couple is used as the redox mediator in DSCs. The I_3^- produced due to regeneration of the dye is reduced at the counter electrode by the reaction:



The CE material is chosen according to the particular application of a DSC. A CE material in a DSC should possess a high catalytic activity and stability towards the electrolyte used in the cell. As a standard choice of material for CE in DSCs, Pt is chosen due to its attractive properties like high catalytic activity, excellent stability towards the iodide redox species, etc.³²⁻³⁴ Since it is an expensive noble metal and of diminishing supply, several kinds of alternative materials like carbon, conducting polymers, transition metals, etc. have been explored and introduced to replace Pt.

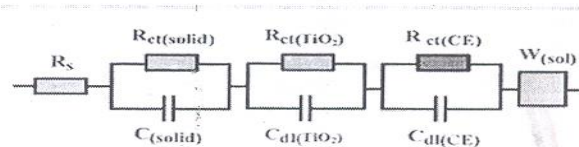


Fig. 3 Equivalent circuit used to represent interfaces in solar cell.³⁵

V. Platinum counter electrode

1. Bulk Pt as counter electrode

Pt is a lustrous, silvery white metal, discovered by Julius Scaliger in 1735, who derived its name from the Spanish word 'platina', which means "little silver". Its excellent physical and chemical properties, such as: (a) stability (does not oxidize) in air or water even at high temperatures, (b)

dissolves in aqua regia, forming chloroplatinic acid (H_2PtCl_6), and (c) good electrical and thermal conductivity, made the material useful in a wide range of applications, such as in vehicles as a catalytic converter, a catalyst in chemical reactions, surgical tools, electrical resistance wires, etc. Compared to the bulk Pt, Pt nanoparticles have excellent characteristic properties like high surface area, high transmittance, low charge transfer resistance, high electrical conductivity and corrosion resistance, better than any other noble metal. These key features made Pt attractive or use as CE/catalytic materials in DSCs.^{35,36}

2. Pt nanoparticles

Platinum (Pt) is the most preferred material for CEs in DSCs, due to its electrocatalytic activity towards I_3^- reduction. The best CE developed for a DSC is Pt sputtered on FTO, which has a thickness around 0.2-2 micron. These CE films show a high electrical conductivity, catalytic activity towards I_3^- , and high reflecting properties.⁴² Other than sputter-coating, there are several other deposition techniques, like pulse-current electrochemical deposition (PED), thermal vapour deposition, spray pyrolysis, etc. which use a large amount of the expensive Pt.³⁷ The main aspects to be considered for CEs in DSCs are optical transparency and low cost. For a transparent film. It nanoparticles can be synthesized by the electrochemical reduction of hexa-chloroplatinate, or by the thermal decomposition of chloroplatinic acid³⁸⁻⁴¹ These alternative methods require only low Pt quantities, around 10-100 mg cm⁻², thus the costs can be reduced⁴³⁻⁴⁴ For a transparent and stable counter electrode, Pt nanoparticles are best, due to their high surface area and higher density of catalytic sites.⁴² A highly transparent Pt CE is an important factor in a DSC mainly for the back-side illumination process; also the reflective property of a Pt film improves the light harvesting efficiency of the dye absorbed onto the 12 nm TiO₂ film, which increases the performance of the cell.⁴¹⁻⁴² Calogero et al.⁴² fabricated a low-cost transparent CE based on Pt nanoparticles by a bottom-up synthetic approach, in which the Pt nanoparticles have a high surface area and homogeneity compared to Pt sputtered CEs. The high surface area of the Pt nanoparticles indicates a large number of active site which are available for the reduction of I_3^- , thus increasing the current density.⁴² From recent studies it was proved that modifying the structural characteristics and facets of Pt enhances its catalytic activity. Recently, 3-D nanostructures with high surface areas emerged as promising materials for CEs. These includes structures like multipods, nanowires, nanoflowers, nanotubes, etc.⁴⁵⁻⁵³ Recently, Jeong et al.⁵⁴ proposed that periodically aligned nanostructures can be used as CEs in DSCs. Jeong et al.⁵⁴ synthesized periodically aligned Pt nanocups (NC) with a controlled diameter (300-600 nm) and pitch size (400-800 nm) for the enhancement of the counter electrode surface area by UV-based nanoimprint lithography (NIL) (Fig.4(a)). Since the nanocups have a large surface area, the electrolyte can contact the inner and outer faces of the cup. Vertically aligned Pt NCs are deposited on top of the Pt-coated FTO.

The physical properties and the photovoltaic parameters were compared against planar Pt.

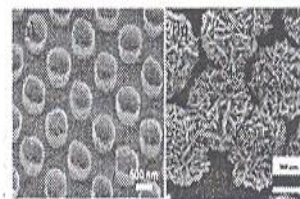


Fig. 4 SEM images of (a) Pt nanocups⁵⁴ (b) Pt nanoflowers.⁴⁵

Scanning electron microscopy (SEM), cyclic voltammetry (CV) and electrochemical impedance spectroscopy (EIS) proved that the Pt NCS have a high surface area, greater catalytic activity towards the I^-/I_3^- redox species and thus, a lower impedance. As the internal resistance, R_{CT} was low; there was an increase in the FF and I_{sc} . Regarding the photovoltaic performance, the DSCs employing Pt NCs showed an efficiency of 9.75%, whereas the planar Pt showed a 7.87% efficiency.⁵⁴ Similarly, several studies have been done to understand the catalytic and photovoltaic behaviour of different Pt facets. Zhang et al.⁵⁵ studied the catalytic reaction of Pt nanoparticles with different exposed facets like (100), (411) and (111) towards the I_3^- reduction by using density functional theory (DFT) and experiments. Fig. 5 shows the transmission electron microscope (TEM) and HR-TEM images of the three Pt facets. From theoretical considerations, the catalytic activity towards the I_3^- reduction was calculated and it was found to be in the order of Pt(111) > Pt(411) > Pt(100). From the EIS analysis curves, the Pt(111) showed a lower charge transfer resistance (around 1.31 Ω cm²) compared to other facets. The photovoltaic performance of the system, shown in Fig. 6, proves that the Pt(111) facets can be equipped as CEs in DSCs, because a DSC with Pt(111) as the CE showed a conversion efficiency of 6.91% with a high current density (16.29 mA cm⁻²) and voltage (757 mV), which are superior over Pt(411) and Pt(100), which gave an efficiency around 6.16% and 5.66%,⁵⁵ respectively.

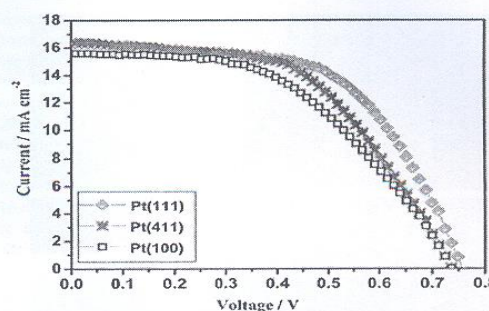


Fig. 6 I-V characteristics of different Pt facets as the CE in DSC.⁵⁵

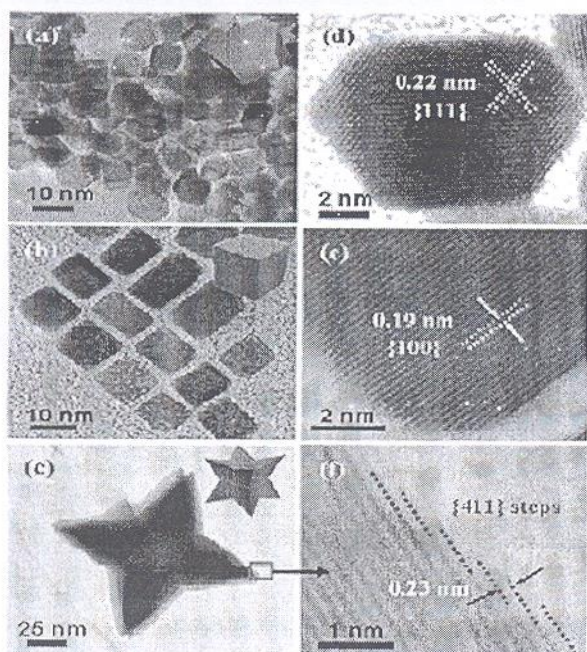


Fig. 5 TEM and HRTEM images of (a and d) Pt (111), (b and e) Pt (411) and (c and f) Pt (100) facets.⁵⁵

3. Pt composite materials

In order to improve the electro catalytic activity of CEs further, Pt in composition with carbon and polymers has been studied. For the first time, Yen et al.⁵⁷ prepared Pt nanoparticles supported on graphene-coated FTO (Pt NPs/GR) by a water ethylene-glycol method⁵⁶ as the counter electrode in a DSC. The physical properties and photovoltaic performance of the Pt NP/GRCE were compared against graphene and Pt films as CE in DSCs. Cyclic voltammetry (CV) measurement, which is a powerful and efficient method to determine the catalytic activity of a material in an electrochemical reaction, indicates that in contrast to the Pt film, the Pt NP/GR possess a higher electron transfer rate, surface area and hydrophilicity, due to the oxygen containing graphene and an enhanced electrocatalytic behaviour towards the I_3^- reduction. Similarly, the EIS measurements have shown that the composite material has a decreased internal resistance (R_{CT}), around $0.67 \Omega \text{ cm}^2$, and a low diffusion resistance (R_d) of $0.023 \Omega \text{ cm}^2$, which increased the FF of the DSC. The SEM and TEM images shown in Fig. 7 (a and b, respectively) give the morphology of the high surface area composite material (Pt NP/GR). Comparing the photovoltaic performance of PT NP/GR with respect to bare Pt, the former showed an efficiency of 6.35%, which is higher than that of the latter, at 5.47%.⁵⁷ Another Pt composite material that worked as a CE material is a Pt NP-MWCNT composite. Huang et al.⁵⁷ synthesized a Pt NP-MWCNT composite by using imide functionalized material, that is poly(oxyethylene) (POEM), a segmented polymer and this composite material was then spin coated as the CE film. The segmented POEM was synthesized by milling the poly(oxyethylene) diamine (POE 2000) and 4,4'-oxydiphthalic anhydride (ODPA). The POE-backed polymer is used

mainly for the non-covalent blending of Pt NPs with MWCNTs for improving the electro-catalytic activity of the composite layer on the CE. The Pt NP-MWCNT composite material showed a higher current density and efficiency of around 8%, due to its good catalytic mechanism towards the I_3^- reduction (the reduction and oxidation peaks are clearly evident from Fig. 8).

The surface morphology examined by the SEM and TEM images is shown in Fig. 7(c) and (d). The TEM image clearly shows the fine attachment of Pt nanoparticle to the MWCNTs.⁵⁸ The main advantage of incorporating the two materials is that the composite material obtains all the physical properties, like electron charge transfer, high specific area, etc., which can enhance the overall performance of the cell.⁵⁷ Even though Pt is the preferred material for a DSC, it also possess some disadvantages, like high cost (~\$1456.55 per Troy ounce at present), low abundance of material, diminishing catalytic property on exposure to dye solution, and stability due to the corrosive nature of the electrolyte (forms PtI_4 , or H_2PtI_6).^{59,60} These characteristics encourage the invention of new conducting materials for the counter electrode, like carbon nanoparticles, CNTs, graphene, carbon black, conducting polymers, transition metals, etc.

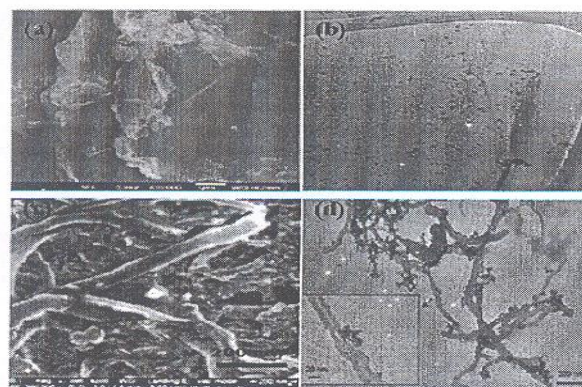


Fig. 7 SEM and TEM images (a and b) Pt NP/GR (ref. 57) (c and d) Pt NP/MWCNT composite structure.⁵⁸

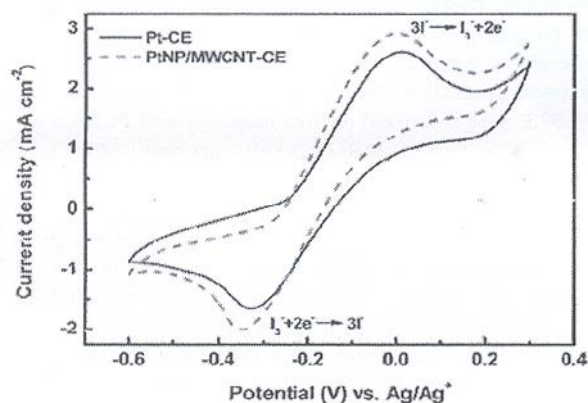


Fig. 8 CV of Pt NP-MWCNT-CE and Pt-CE in 0.01 M I_2 , 0.001 M I_3^- and 0.1 M $LiClO_4$ in AN, at a scan rate of 100 mV s^{-1} .⁵⁹

VI. Carbon materials

For a low-cost OSC, we have to utilize a cheap and abundant material in the Earth's crust as the material for the counter electrode, which can take the role of the Pt in DSCs. Carbon, which is the sixth most abundant material in the Earth's crust, is the best material to replace Pt. Mainly due to its core features like cost-effectiveness, environmental friendliness, availability, corrosion resistance and excellent catalytic activity towards the redox species, carbon is an attractive option. Carbon black, activated carbon, mesoporous carbon, carbon nanotubes (CNTs), graphene and fullerenes, all belonging to the carbon family, have been used as alternative materials for Pt in the CE.³¹ Even though carbon is not as good as Pt, its performance in a solar cell can be improved by employing a porous film with a high surface area. It was in the year 1996, that for a monolithic DSC, Kay and Gratzel used a mixture of graphite and carbon black, which acted as a catalyst as well as a lateral current collector by replacing the expensive Pt coated FTO substrate and simplified the manufacturing process. The cell showed an overall efficiency of 6.7%.⁶¹

I. Carbon black

Carbon black, which is mainly produced by the incomplete combustion of petroleum products is widely used in industry for printing toners. Carbon black is an excellent material for a counter electrode, due to its properties like high surface area-to-volume ratio, excellent conductivity and the electrocatalytic activity towards the I^-/I_3^- redox species.⁶²⁻⁶⁴ In carbon materials, the active sites for catalysis are located at the crystal edges. When a carbon material is used as the CE, there must be a control of the layer thickness, because it affects the catalysis and resistance of the material. Murakami et al.⁶⁵ worked on varying the thickness of the carbon black as the CE material (Fig. 9(a)).

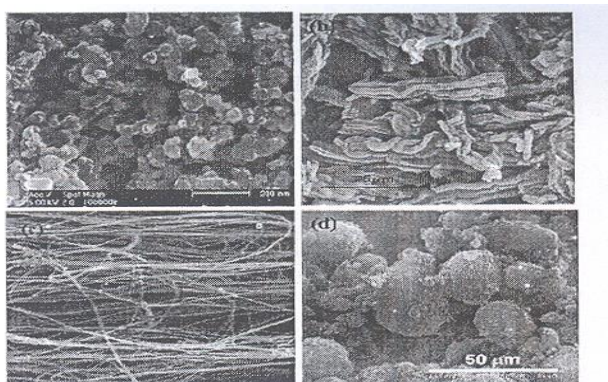


Fig. 9 SEM images of different carbon morphologies (a) carbon nanoparticles,⁶⁵ (b) large mesoporous carbon,^{66a} (c) MWCNTs webs,¹⁰⁷ (d) carbon nano-onions.^{66b}

It was found that the FF of the cell increases as the thickness of the carbon film increases; similarly the charge transfer resistance of the CE decreases, which indicates that a thick carbon black CE possess a high catalytic activity which improves the overall cell performance. It was observed that a film of thickness 14.47 μm showed an efficiency of 9.1%,

with an excellent current density and voltage. From the EIS spectra it was confirmed that the high surface area carbon black has a low charge transfer resistance, around 2.96 Ωcm^2 , which makes carbon black a low-cost and corrosion free CE.⁶⁵

Normally, a transparent conducting oxide, like FTO or ITO, is used as DSC substrates. For a low-cost CE, we have to use a low-cost catalyst in addition to a low-cost substrate like stainless steel or nickel.³¹ Metal substrates are not preferred in liquid state DSCs, because of the corrosive nature of the I^-/I_3^- electrolyte. Carbon is a promising, anti-corrosive substrate and it provides a large FF and low sheet resistance. The mainly used stainless steel substrates are SUS-316 and SUS-304, due to their high corrosion resistance, compared to other stainless steel substrates. Coating a carbon catalyst on SUS-316 and SUS-304 made them eligible to be used as CEs in DSC and an overall efficiency of 9.15% and 8.86%, respectively, were obtained.³¹

2. Mesoporous carbon

Mesoporous carbon materials have received the greatest attention amongst all carbon materials, due to their large internal surface area, pore volume, tuneable and narrow pore diameter, etc. The most commonly used method for developing mesoporous carbon structures is a templated synthesis, which is also known as nanocasting. By using this method, the fabricated material can have homogenous and interconnected pores.⁶⁶ Large porous carbon (LPC) structures were used as CEs in DSCs (see Fig. 9 for the SEM images). From the nitrogen adsorption isotherm measurement, it was observed that the material possess a high surface area and pore volume compared to a mesoporous silica material (a high specific area of 1300 m^2g^{-1}). The high surface area of the LPC helps in the penetration of the electrolyte, which resulted in giving an efficiency of around 7.1%, which was more than that for an activated carbon as the CE.^{66a} By using different morphologies of carbon structures, which have a high surface area, like carbon nano-onions as the CE, shown in Fig. 9(d), this can reduce the cost of the CE and improve the DSC performance.

3. Graphene

One single atomic thick layer of the mineral graphite, called graphene, became a subject of intense research after its discovery in 2004.⁶⁷ It is typically a two-dimensional (2-D) sheet, composed of hexagonally arrayed sp^2 carbon atoms, that form a honeycomb lattice structure. As the thinnest material, it possesses many unusual properties, like high carrier mobility ($\sim 10000\text{ cm}^2\text{ V}^{-1}\text{ s}^{-1}$),⁶⁷⁻⁶⁹ high specific area ($2630\text{ m}^2\text{ g}^{-1}$),⁷⁰ excellent thermal conductivity ($\sim 3000\text{ W m}^{-1}\text{ K}^{-1}$),⁷¹ high Young's modulus ($\sim 1\text{ TPa}$),⁷³ and high optical transparency (97.7%).⁷³ Graphene is a promising material to replace Pt in DSCs, due its excellent conductivity and high specific area that decrease the charge transfer resistance (R_{CT}). Different techniques are used to produce graphene

nanosheets (GN)-based CEs for DSCs. The most efficient method to produce GNs is by the oxidative exfoliation of graphite, followed by hydrazine reduction; the maximum obtained efficiency for this process is 6.8%. This method also reveals the fact that the annealing temperature for GNs is an important factor, which results in a high efficiency. The optimized temperature is about 400°C and above that the GNs will peel-off from the substrate due to the presence of some organic binders." Various other techniques are also available to prepare graphene CEs, by the chemical reduction of graphene oxide colloids under microwave irradiation,⁷⁵ electrophoretic deposition (EPO) followed by annealing,^{76,77} thermal exfoliation from graphite oxide (GO), etc.⁷⁸ The DSC performance with graphene as the CE depends upon the structure of the graphene. Extremely pure graphene has an excellent conductivity, but possesses a limited number of active sites for the I⁻/I₃⁻ electrocatalytic mechanism. Kavan et al.⁷⁹ proved that the electrocatalytic activity of GNs is mainly associated with the defects and oxygen containing functionalized groups present in them. The GN prepared from graphite by an oxidation-reduction approach contains lattice surface defects and these lattice defects are considered as the electrocatalytic active sites.⁷⁹ Roy-Mayhew et al.⁸⁰ found that the electrocatalytic activity towards the I₃⁻ reduction can be increased by increasing the number of oxygen containing functional groups in the graphene sheet. On the other hand, Xu et al.⁸¹ reported that reduced graphene oxide (RGO) functionalized with the -NHCO- group exhibited a higher catalytic activity than the original RGO, indicating that -NHCO- groups can increase the catalytic activity."

4. Graphene-based composite materials

(a) Graphene-polymer composite. Graphene-based composite materials captured attention from 2006 onwards, when the first work on graphene with conducting polymers was reported by Stankovich et al.⁸² Mostly, in graphene polymer composite films, the polymer acts as a conducting support and the graphene is responsible for the high catalytic activity towards the reduction of I₃⁻. Furthermore, graphene sheets can also be used as a support for conducting polymers and this is done by dispersing the conducting polymers on the graphene sheets. Normally, the conducting polymers used are polyaniline (PANI) and poly(3,4-ethylenedioxythiophene) (PEDOT). Wang et al.⁸³ synthesized a nanocomposite material with PANI-graphene sheets by an in situ polymerization technique. From the SEM image, shown in Fig. 10(b), it can be observed that the graphene sheets were homogeneously coated on the PANI. The DSC of the graphene- PANI nano-composite gave an efficiency of around 6.09%, which was close to that of using a bulk Pt CE, which gave an efficiency around 6.88%." Similarly, the Cf prepared by Lee et al.⁸⁴ consisting of a PEDOT-graphene composite material, gave an efficiency of 6.26%, mainly due to the high loading of graphene into the PEDOT, higher electronic charge transfer and electrochemical activity.⁸⁴ Graphene films can be well-dispersed in (3,4-ethylenedioxythiophene) poly

(styrenesulfonate), that is a PEDOT-PSS matrix, due to a strong static interaction between 1-pyrenebutyltyrte (PB⁻) functionalized graphene sheets and the PEDOT chains, which is clearly evident from Fig. 10(a).⁸⁵

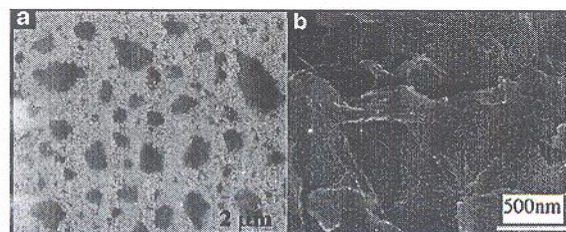


Fig. 10 SEM image of (a) graphene-PEDOT-PSS composite⁸⁵ (b) graphene-PANI composite.⁸⁵

(b) Graphene-metal composite. To reduce the amount of Pt loading in DSCs, there is a need to exploit graphene composite nanostructures. Metals, like nickel (Ni) and cobalt (Co), can be combined with graphene to form a composite CE. Dou et al.⁸⁶ synthesized a Ni₁₂P₅-graphene composite as a CE material for DSCs by a hydrothermal method. This material shows a fine electrocatalytic activity towards the I₃⁻ reduction, giving an efficiency of 5.7%. The main advantage of using a metal-graphene composite as a CE is that these composite materials will increase the electron transfer rate at the CE, act as an active site for the electrocatalytic process and also act as a spacer between the graphene sheets, which speeds up the diffusion of the electrolyte, whereas the graphene provides a fast diffusion pathway for the electrolyte by creating a brilliant electrode-electrolyte contact, which improves the electron transfer rate at the electrolyte-CE interface.^{87,88} Fig. 11 shows the SEM and TEM images of a Ni NP-graphene composite structure. Similarly, by using a Pt-graphene composite material (Fig. 11(d) shows the SEM image of the Pt-graphene structure) on DSC, Gong et al." reported an efficiency of 7.66%, which was lower than that of a Pt sputtered CE, mainly due to the reduced loading of platinum. Further research by Bajai et al.³⁹ revealed that the Pt loading has an important role in improving the overall performance of the cell.^{89,90} The mechanism of the electron transport in a graphene-metal composite material is schematically shown in Fig. 12. Recently, it was found that tungsten carbide (wc) can form a composite material with graphene nanosheets (GN) which is another alternative composite material for the CE. Tungsten carbide is used, since it has a Pt-like catalytic behaviour, high stability and low resistance.^{94,95} A WC-GN composite material for a DSC yielded an efficiency of 5.88%, with a high current density and fill factor. This is because of some important aspects of the WC-GN composite, such as: (a) the wc nanoparticles and GN are uniformly

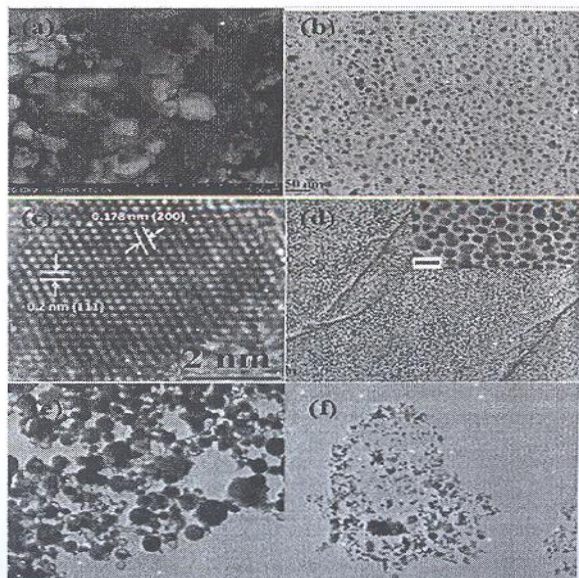


Fig. 11 SEM image of (a) Ni₁₂P₅-graphene composite⁸⁶ (d) Pt-graphene composite⁸⁹ and HRTEM image of (b) Ni NP on graphene sheets (c) high resolution image showing the lattice planes of Ni nanoparticles.⁸⁷ (e) Tungsten nanoparticle,⁹⁶ (f) WC-GN composite.⁹⁶

dispersed, thus providing a large surface area on the electrode, which benefited the transport of electrolyte, (b) as the surface area increases, the electrochemical activity also increases, and (c) the strong adhesion of the WC-GN composite material, supported by a low resistance at the electrolyte-CE interface, which increases the FF.⁹⁶ The WC-GN composite is a potential low-cost material to replace the expensive Pt.

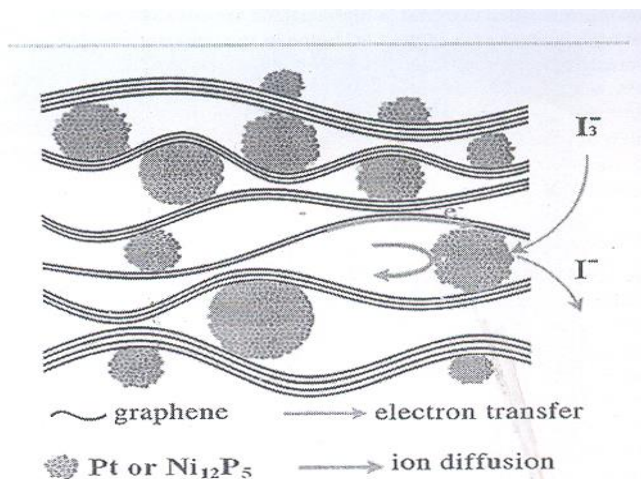
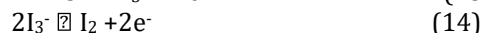


Fig. 12 Electron transport mechanism in a graphene-metal composite.⁸⁶

(c) Graphene-carbon Composite. As we have already seen, graphene is a promising candidate for photovoltaic applications, due its high hole-transport mobility, inertness against oxygen and water, etc. Due to the advantages of graphene and CNTs, Choi et al.⁹¹ developed MWCNTs-graphene as a CE for DSCs. Here, MWNTs were deposited on top of the graphene layer using the chemical vapour deposition (CVD) technique. The composite structure

showed an excellent electrocatalytic property compared to graphene and the MWNTs alone CEs. The I-V characteristic of the OSC with MWNTs-graphene CE is shown in Fig. 13. The cell exhibited a maximum efficiency of 3% with a current density of 5.6 mA cm⁻² and a voltage of 0.76 V which was higher than that of the DSC with a MWNTs CE. The overall increase in efficiency was mostly due to the expansion of the reaction area at the interface, due to the vertically grown MWNTs on the graphene sheets. The main disadvantage of this process was the complicated synthesis route and high production cost.⁹¹

By using a facile method, Banumur et al.⁹² prepared a MWNT-graphene nanosheet (GNS) composite material for a CE. The physical properties and photovoltaic performance was observed in comparison to graphene and MWNTs CEs. From the cyclic voltammograms, the CE composed of MWCNTs, graphene, and MWNTs-graphene have shown two characteristic redox peaks which can be assigned as:



This implies that all three electrodes have an excellent electrocatalytic activity towards the I⁻/I₃⁻ redox couple and a better understanding about the composite material was given by the EIS spectra, which signified that there is a marginal reduction in the R_s and R_{CT} values for the MWNTs-GNS composite material, compared to others. A composite material containing 60% of MWNTs and 40% graphene gave an overall efficiency of 4%.⁹² Another MWCNT-

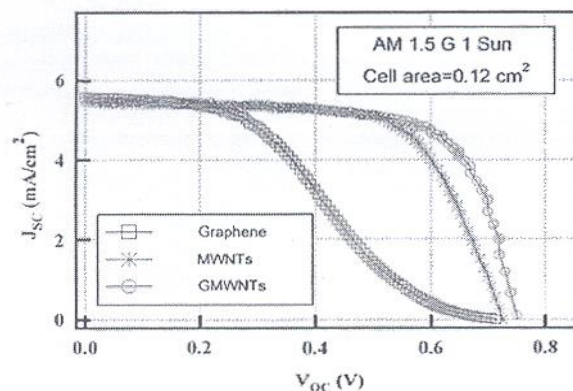


Fig. 13 I-V characteristics of DSCs with graphene, MWNTs, and GMWNTs as CE.⁹¹

graphene composite for a CE was fabricated by Velten et al.⁹³ which exhibited a high conversion efficiency of 8.82%, indicating that there is an increase of the electrical conductivity between the MWCNT bundles and the graphene sheets when they are made into a composite.⁹²

5. Carbon nanotubes (CNTs)

Carbon nanotubes (CNTs), which are an allotrope of carbon, captured the attention of the scientific community after their

discovery in 1991.⁹⁷ Nanotubes consist of concentric graphitic cylinders at either ends and they align naturally into ropes and are held together by van der Waals forces. CNTs are the only form of carbon which has extended bonding and no dangling bonds. CNTs are also known as tubular fullerenes or 'Bucky tubes', as they are derived from fullerenes. CNTs can be classified into three structures due to their number of rolled walls; they are single-walled carbon nanotubes (SWCNTs), multi-walled carbon nanotubes (MWCNTs) and double-walled carbon nanotubes (DWCNTs). CNTs are attractive due to their outstanding properties, like high electrical conductivity, thermal conductivity and mechanical properties, which are similar to graphene.⁹⁸⁻¹⁰⁰ CNTs possess different structures like CNT bundles, a vertically-aligned CNT forest, a random network of interconnected CNTs, horizontally aligned CNTs, etc.¹⁰¹ These structures have an effect on the behaviour of a film in a device. The most commonly used CNT-based CE consists of a random network type of film. These films have a high sheet resistance ($50 \Omega \text{ cm}^{-2}$) even though the films are transparent and very thin. CNTs are catalytically active towards the redox species in a DSC.¹⁰²⁻¹⁰⁶ Similarly, SWCNT and MWCNT structures are used in DSCs due to their exciting properties like electrical conductivity, extremely large and tuneable surface areas and controllable defect edges that could facilitate the electron kinetics associated with I_3^- reduction. Noureldine et al.¹⁰⁷ synthesized MWCNT webs, which consisted of 20 layers (Fig. 9(e)) as a counter electrode material in a DSC, which contains a different electrolyte of 1-methyl-3-propylimidazole-2-thione (T) and 2,2'-dithiobis(1-methyl-3-propyl-2-imidazolium) ditriflate (DT). The cell covered an efficiency of 4.2% and 20 layers of MWCNT webs as the CE has a higher surface area and good electrocatalytic activity towards the new electrolyte, compared to Pt.¹⁰⁷ Core-shell structures of CNTs are also used as the CE material in DSCs. Shin et al.¹⁰⁹ synthesized highly conductive and thermally stable CNT-PEDOT core-shell nanostructures by a modified emulsion polymerization technique. CNT-PEDOT core-shell structures as the counter electrode in DSCs showed an efficiency of 4.62% with a high fill-factor. Moreover, the coreshell nanostructures exhibited a higher thermal stability and electrical conductivity, compared to pure PEDOT.¹⁰⁸⁻¹¹⁰

VII. Polymer materials

Conducting polymers are spectacular materials that can be used as CEs in DSCs. A conducting polymer has the potential to replace Pt because of its high electrochemical activity. The most preferred conducting polymer is PEDOT, due to its high stability, electrochemical activity, transparency and stability.¹¹¹⁻¹¹³ Other polymers such as polypyrrole (PPy), polyaniline (PANI) and PEOOT doped with p-toluenesulfonate (PEOOT-TsO) or polystyrenesulfonate (PEDOT-PSS), etc. can also be used for the same.¹¹⁴⁻¹¹⁸ In 1998, Yohannes and Inganas reported that electrochemically polymerized and doped poly(3,4-ethylenedioxythiophene) PEDOT can catalyze the reaction of the redox couple (I^-/I_3^-) in a DSC.¹¹⁹ A cost-effective conducting material exhibiting a

high catalytic activity should be used simultaneously to act as a catalyst for the I_3^- reduction and charge transport. Lee et al.¹²⁰ synthesized a PEDOT CE for a DSC, without a TCO, by an in situ polymerization method. The PEDOT had a thickness of 60 nm, and an $\sim 88\%$ transmittance. The CV curve of PEDOT coated on a glass substrate showed a higher peak compared to Pt, indicating that PEDOT CEs are electrochemically active and possess a higher transfer rate on PEDOT even though the PEDOT CE has no TCO substrate. The PEDOT CE in a DSC showed an efficiency of 5.08%. By increasing the electrical conductivity of the PEDOT, the photovoltaic performance can be increased further.¹²⁰ Fig. 14 shows the schematic diagram of a DSC with a PEDOT CE.

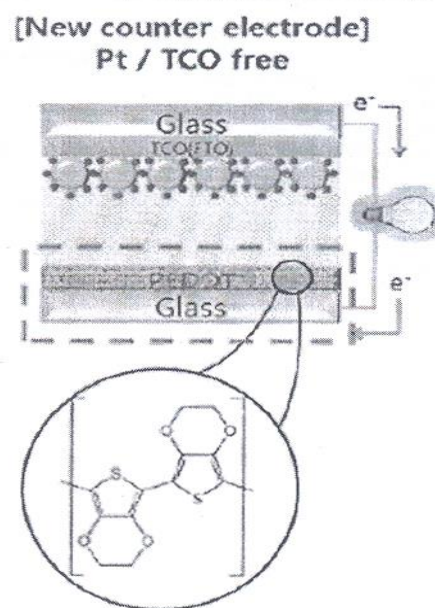


Fig. 14 Schematic diagram of a DSC with PEDOT as the CE without a TCO.¹²⁰

Recently Tang et al.¹²¹ synthesized Ppy and PANI nanostructures by chemical and electrodeposition techniques and observed that the double-layered PANI consisting of a nanoparticle- and a nanofiber-layer formed by electrodeposition, when used as a CE material for DSC, showed an efficiency of 6.58% compared to the chemically deposited PPy nanostructures. Fig. 15 shows the SEM image of a double-layered PANI CE and PPy CE. The enhanced efficiency is due to the excellent properties of the PANI double layer structure such as (a) high surface area and porous structure, (b) capacity to load electrolyte, (c) more active sites for charge transfer and (d) an excellent electrocatalytic activity towards the I^-/I_3^- redox species. A comparison of the photovoltaic performance of the electrodeposited and chemical deposited PANI and PPy are shown in Fig. 16 where the electrodeposited PANI gave a current density of 13.4 mA cm^{-2} and a voltage of 0.728 V.¹²¹

1. Polymer composite material

(a) Polymer-carbon composite. To increase the electrical conductivity of PEDOT further, Lee et al.¹²² prepared another

CE for a DSC with graphene over-coated on a PEOOT film on a flexible target substrate. The high conductivity of the graphene layer decreases the surface resistance and the PEDOT takes the role of the Pt and the TCO. The composite material has shown a transmittance of 70% at 500 nm and also the film has a good mechanical flexibility. Fig. 17(a) represents the structure of a DSC with a graphene-PEDOT CE, and Fig. 17(b) reveals the AFM image showing the surface roughness of the graphene-PEDOT CE. The photovoltaic performance was also increased compared to the bare PEOOT CE.¹²² Polypyrrole and polyaniline can be used with carbon black as a composite material for a CE. Here, the carbon black acts as an interface between the polypyrrole/CE to improve the charge exchange and hence the FF and efficiency will be increased.^{123,124}

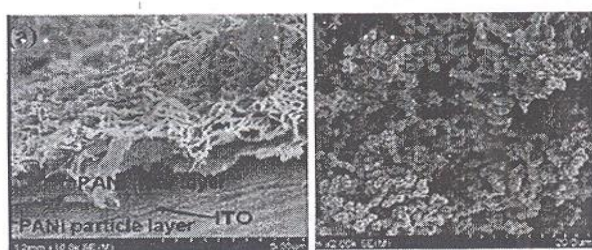


Fig. 15 SEM image of (a) double layer PANI nanostructure by electrodeposition (b) PPy nanostructure by chemical deposition.¹²¹

(b) Polymer-Pt composite. For roll-to-roll manufacture and to produce light weight DSC modules, a flexible substrate is a must. Ma et al.¹²⁵ deposited PI by sputtering on an ITO substrate coated with poly(ethylene naphthalate) to achieve a plastic substrate. By using this substrate as the CE, the DSC showed an efficiency of 5.39% with a high fill factor of 60%.¹²⁵ Wei et al.¹²⁶ used polyvinylpyrrolidone (PVP)-capped Pt on an ITO substrate. This CE material gave a very

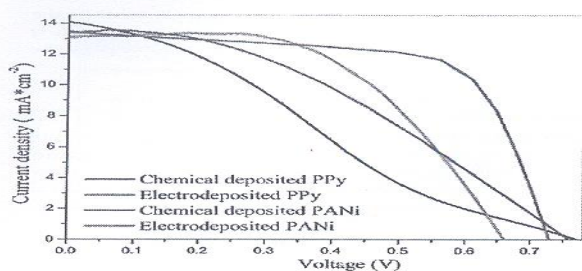


Fig. 16 I-V performance of chemical and electrodeposited PANI and PPy nanostructures.¹²¹

low efficiency of 2.48%, mainly due to the high charge transfer resistance of the material, which decreases the overall performance of the cell.¹²⁶ Conducting polymers like PANI can also be used with Pt. Peng et al.¹²⁷ prepared a PANI-Pt composite material as the CE. In this composite, the Pt nanoparticles, of size 1.5 nm, were well-dispersed with a low loading of Pt (1.1 $\mu\text{g cm}^{-2}$) and gave a flexible CE, which has shown a high conversion efficiency compared to sputtered Pt.¹²⁷

VIII. Alternative materials

Other than carbon, graphene, and polymer CE materials, there are many more alternative materials which are easily and economically available to replace Pt. These include materials like cobalt sulfide (CoS), nickel sulfide (NiS), nickel nitride (NiN), molybdenum sulfide (MoS), molybdenum phosphide (MoP), nickel phosphide (Ni_5P_4), transition metal carbides (TMCS), transition metal nitrides (TMNS), transition metal oxides (TMOs), transition metal sulfides (TMSS), etc.¹²¹⁻¹³¹

1. Transition metal sulfides

These inorganic compounds find favour within DSCs, due to their characteristic features, like wide variety of materials, simple fabrication proceeds and plasticity. Recently Hou et al.¹³² explored low-cost semiconducting materials as the counter electrode and found that rust $\alpha\text{-Fe}_2\text{O}_3$ nanocrystal with (012) and (104) facets is an interesting material for a CE in DSGs. By using the density functional theory (DFT) it was proven that the Fe_2O_3 (012) facet exhibits an excellent adsorption of I^- which is almost similar to the Pt(111) facet, indicating that the $\alpha\text{-Fe}_2\text{O}_3$ has a high electrochemical activity. The material possesses a sheet-like morphology, which is shown in the SEM and TEM images in Fig. 18(c) and (d), respectively.¹³² The photovoltaic performance of $\alpha\text{-Fe}_2\text{O}_3$ was almost comparable to Pt and is clearly evident in Fig. 19. $\alpha\text{-Fe}_2\text{O}_3$ as the CE in a DSC gave an efficiency of 6.96%. A low current density was obtained for $\alpha\text{-Fe}_2\text{O}_3$ mainly due to the high resistance for electron transport owing to the thick film used. Ferric oxide materials have a superiority over the other existing CE materials in terms of their high abundance, non-toxicity, and superior efficiency and therefore this is an excellent material to replace the expensive Pt.¹³²

Transition metal sulfides are one of the promising materials which are capable of replacing Pt and under this category CoS, MoS_2 , and WS_2 have potential, due to their excellent electro-catalytic activity for the reduction of I_3^- , and availability in plentiful and cheaper feedstock than Pt.¹³² Kung et al.,¹³⁴ used one dimensional CoS acicular nanorod arrays (ANRAS) as a CE material in a OSC and obtained an overall efficiency of 7.67%. Fig. 21(e) and (f) show the SEM and TEM images, respectively, of CoS ANRAS. The long term stability of the film in the electrolyte was studied by cyclic voltammetry (CV), which revealed that the CoS ANRAS had an excellent catalytic activity towards the I^-/I_3^- electrolyte.¹³⁴ Due to its excellent electrocatalytic activity, CoS has also been extensively used in other applications, such as electrochemical capacitors, cathodes for lithium ion batteries, etc. Different morphologies of CoS nanostructures were synthesized, like 3-D nanospheres, 2-D nanoflakes, etc. in order to enhance the electrocatalytic activity.¹³⁵⁻¹³⁷ Similarly, molybdenum sulfide (MoS_2) is considered as one of the best candidates for a CE material, because of its analogous structure to that of graphene. Little work has been done on MoS_2 as a CE material. WU et al.¹³⁸ worked on tungsten sulfide (WS) and MoS_2 materials for the CE in DSCs

and obtained an efficiency of around 7.73% and 7.59%, respectively.¹³⁸ Further studies showed that by adding carbon materials to MoS₂, the electrocatalytic activity of the CE can be increased. Different composite materials like WC, MoC, MoS₂-graphene, etc. have been used in DSCs as CEs and obtained good performances.¹³⁹⁻¹⁴¹ Yue et al.¹⁴² prepared a highly porous molybdenum sulfide-carbon (MoS-C) hybrid film for a CE by a hydrothermal route. The MoS₂ had a lamellar structure and the MoS-C hybrid composed of many interlaced nanosheets, as shown in Fig. 18(a) and (b). The EIS spectra and CV curve indicate that the R_{CT}

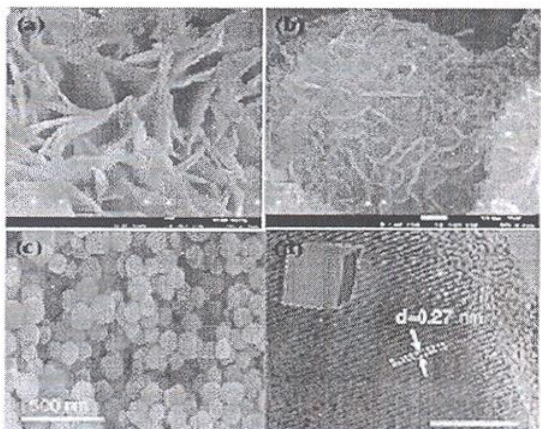


Fig. 18 SEM image of (a) MoS₂,¹⁴² (b) MoS-C,¹⁴² (c) α -Fe₂O₃,¹³² (d) TEM image of α -Fe₂O₃.¹³²

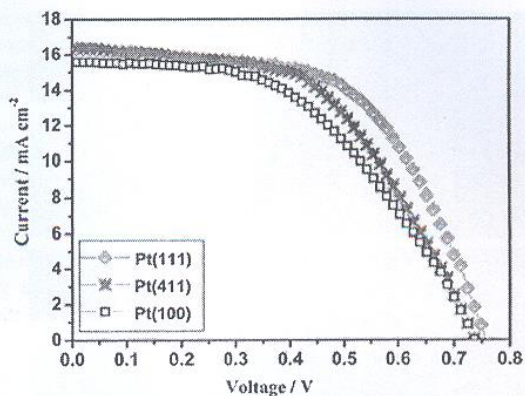


Fig. 6 I-V characteristics of different Pt facets as the CE in DSC.⁵⁵

decreases with increasing carbon content in the hybrid film and it also possess a high electrocatalytic activity and faster reaction for the I₃⁻ reduction, due to the high surface area of the film and the presence of the carbon content within it. Due to all these properties of the MoS-C composite, the use of the same resulted in giving an efficiency of 7.69%. From the IPCE spectra (Fig. 20) it is clear that the highly porous MoS₂-C as a CE exhibits the highest photoelectric response of 67.3% at 520 nm, which is higher than that from a Pt CE, whose response was 60.9% at the same condition.¹⁴²

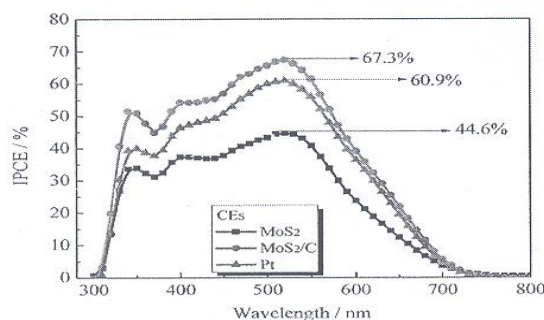


Fig. 20 IPCE spectra of DSC using MoS₂-C as the CE compared with Pt, MoS₂.¹⁴²

2. Transition metal carbides/nitrides/oxides

Transition metal carbides and nitrides are potential substitutes for a Pt CE due to their low cost, high catalytic activity and good thermal stability. Wu et al.¹⁴⁵ studied the electrocatalytic behaviour and the overall cell performance of the three classes of nanoscaled transition metal carbides, nitrides and oxides as the CE material in a DSC. They have exciting properties, like durability towards the covalent solid, high melting temperature of the ionic crystal, electrical and thermal conductivities of the transition metal and most striking one is the platinum-like catalytic activity.^{143,144} The catalytic activity is determined by the electronic structure of the catalyst, as well as the electronic structure of the host metal. It can be modified by a foreign atom (C or N) through the electron transfer process in either way: that is from the host to an interstitial atom, or from the interstitial atom to the host metal. TMCs and TMNs shows excellent catalytic activity because they contain a small atom, such as carbon or nitrogen, inserted interstitially in their lattices, producing a series of TMCs and TMNs with unique properties. Some materials like chromium carbide (Cr₃C₂), vanadium nitride (VN), titanium carbide (TiC) (see fig. 21(a)-(d) for their SEM images), etc. showed a high catalytic activity towards the reduction of I₃⁻. A high power conversion efficiency of 7.63% was obtained when highly conducting mesoporous carbon was added to the vanadium carbide material, thereby forming a vanadium carbide composite (VC-MC) material (fig. 22 shows the I-V curve of the VC-MC in comparison with other carbides and PI). This study reveals that by combining a high catalytically active material (VC) and a high electrically conducting material (MC), the catalytic activity of the CE can be improved significantly. The carbides showed an outstanding stability and a better catalytic activity than PI for the regeneration of the new organic redox couple of di-5-(1-methyltetrazole)disulfide 5-mercapto-1-methyltetrazole N-tetra methyl ammonium salt T₂/T.¹⁴⁵ All these materials can be considered as optional materials (instead of Pt) as CEs in DSCs.

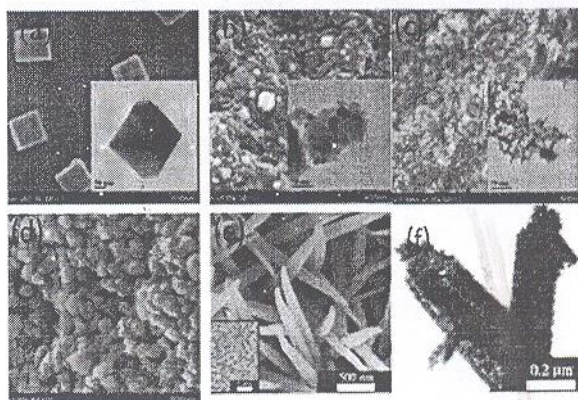


Fig. 21 SEM images of (a) VC(N) (b) VC-MC (c) TiN (d) TiC(N)¹⁴⁵ (e) CoS (ANRAs), TEM images (a-c) shown inset and (f) CoS (ANRAs).¹³⁴

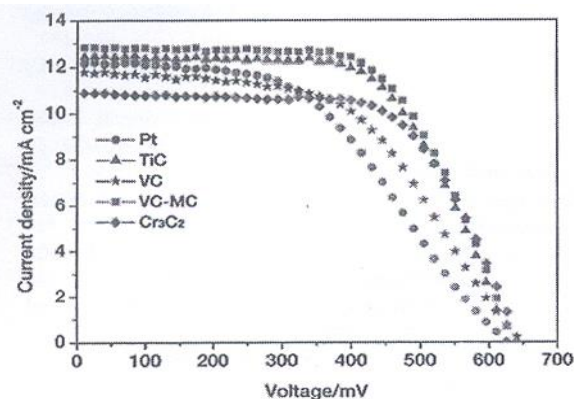


Fig. 22 I-V curve of transition metal carbides in comparison to Pt.¹⁴⁵

IX. Conclusions and Prospects

The efficiency of DSCs is approaching the efficiency level needed for commercialization. The present review gives a vivid account of the materials used as CEs in DSCs. An excellent CE material should possess (a) perfect stability and (b) high catalytic activity and Pt holds these two properties, that is the reason it holds the title of the best counter electrode material. However, Pt is an expensive noble metal and for the worldwide commercialization of DSCs, this needs to be replaced with inexpensive materials. Several materials such as carbon nanostructures, activated carbon, CNTs, graphene, conducting polymers, etc. and their various combinations were used as CE materials and recently transition metal carbides, nitrides, sulfides and oxides were also evaluated as CE materials due to their availability, plasticity and simple fabrication procedures. Organic and inorganic materials possess both advantages and disadvantages. Carbon compounds and conducting polymers are cost effective materials compared to Pt; also these materials show excellent electrochemical activity towards the redox species, but adhesion towards the TCO substrate poses a long term stability issues. Similarly, transition metal compounds have a tremendous catalytic activity towards the triiodide/iodide redox species and to T_2/T^- , but the electron transport between the nanoparticles and conducting substrate is low and this hinders the overall performance of the DSCs. However, this drawback could be overcome by incorporating carbon nanostructures to the transition metal compounds, which will improve the catalytic performance of the non-noble metals. Thus, the development and evaluation of new organic and inorganic compounds as an alternative material to Pt in DSCs is a promising research area, which is essential to reduce the cost of the devices for commercialization.

References:

- 1 B. O'Regan and M. Gratzel, *Nature*, 1991, 353, 737-740.
- 2 W. West, *Proc. Vogel Cent. symp., Photogr. Sci. Eng.*, 1974, 18, 35-48.
- 3 J.N. Moser, *Monatsh. Chem.*, 1887, 8, 373.
- 4 H. Gerisher and H. Tributsch, *Ber. Bunsen. Phys. Chern.*, 1968, 72, 437-145.
- 5 H. Tributsch and H. Gerisher, *Ber. Bunsen. Phys. Chern.*, 1969, 73, 251-260.
- 6 S. Namba and Y. Hishiki, *J. Phys. Chem.*, 1965, 69, 774-779.
- 7 H. Gerischer, M. E. Michel-Beyerle, F. Rebenstroff and H. Tributsch, *Electrochim. Acta*, 1968, 13, 1509-1515.
- 8 M. T. Spitler and M. Calvin, *J. Chem. Phys.*, 1977, 66, 4294-4305.
- 9 M. Gratzel and J. R. Durrant, in *Series on Photoconversion of Solar Energy: Nanostructured and Photoelectrochemical Systems for Solar Photon Conversion*, ed. M. D. Archer and J. Arthur, Imperial College Press, Nozick, 2008, vol. 3, pp. 503-536.
- 10 A. Kongkanand, R. Martine-Dominguez and P. V. Kamat, *Nano Lett.*, 2007, 7, 676-680.
- 11 P. Brown, K. Takeuchi and P. V. Kamat, *Phys. Chem. C*, 2008, 112, 4776-4782.
- 12 (a) D. Li and Y. N. Xia, *Nano Lett.*, 2003, 3, 555-560; (b) E. Hosono, S. Fujihara, K. Kakiuchi and H. Imai, *J. Am. Chem. Soc.*, 2004, 126, 7790-7791.
- 13 (a) C. T. Dinh, T.-D. Nguyen, F. Klein and T.-O. Do, *ACS Nano*, 2009, 3, 3737-3743, (b) G. K. Mor, K. Shankar, M. Paulose, O. K. Varghese and C. A. Grimes, *Nano Lett.*, 2006, 6, 215-218.

14 (a) W. Hu, L. Li, G. Li, C. Tang and L. Sun, *Cryst. Growth Des.*, 2009, 9, 3671-3676; (b) J. M. Wu, H. Huang, M. Wang and A. Osaka, *J. Am. Ceram. Soc.*, 2006, 89, 2660-2663.

15 (a) J. Polleux, N. Pinna, M. Antonietti and M. Niederberger, *Adv. Mater.*, 2004, 16, 436-439; (b) P. Wen, H. Itoh, W. Tang and Q. Feng, *Langmuir*, 2007, 23, 11782-11790.

16 (a) H. Wang, W. Shao, F. Gu, L. Zhang, M. Lu and C. Li, *Inorg. Chem.*, 2009, 48, 9732-9736; (b) X. Peng and A. Chen, *Adv. Funct. Mater.*, 2006, 16, 1355-1362.

17 A. Hagfeldt, G. Boschloo, L. Sun, L. Kloo and H. Pettersson, *Chem. Rev.*, 2010, 110, 6595-6663.

18 M. Gratzel, *J. Photochem. Photobiol., C*, 2003, 4, 145-153.

19 J. B. Asbury, R. J. Ellingson, H. N. Ghosh, S. Ferrere, A. J. Nozik and T. Q. Lian, *J. Phys. Chem. B*, 1999, 103, 3110-3119.

20 G. Ramakrishna, D. A. Jose, D. K. Kumar, A. Das, D. K. Palit and H. N. Ghosh, *J. Phys. Chem. B*, 2005, 109, 15445-15453.